



UNIVERSITY OF LEEDS

This is a repository copy of *Biomechanical Analysis of Infectious Biofilms*.

White Rose Research Online URL for this paper:
<http://eprints.whiterose.ac.uk/100188/>

Version: Accepted Version

Article:

Head, D (2016) Biomechanical Analysis of Infectious Biofilms. *Advances in Experimental Medicine and Biology*, 915. pp. 99-114. ISSN 0065-2598

https://doi.org/10.1007/978-3-319-32189-9_8

Reuse

Unless indicated otherwise, fulltext items are protected by copyright with all rights reserved. The copyright exception in section 29 of the Copyright, Designs and Patents Act 1988 allows the making of a single copy solely for the purpose of non-commercial research or private study within the limits of fair dealing. The publisher or other rights-holder may allow further reproduction and re-use of this version - refer to the White Rose Research Online record for this item. Where records identify the publisher as the copyright holder, users can verify any specific terms of use on the publisher's website.

Takedown

If you consider content in White Rose Research Online to be in breach of UK law, please notify us by emailing eprints@whiterose.ac.uk including the URL of the record and the reason for the withdrawal request.



eprints@whiterose.ac.uk
<https://eprints.whiterose.ac.uk/>

Biomechanical analysis of infectious biofilms

David Head

Abstract The removal of infectious biofilms from tissues or implanted devices and their transmission through fluid transport systems depends in part of the mechanical properties of their polymeric matrix. Linking the various physical and chemical microscopic interactions to macroscopic deformation and failure modes promises to unveil design principles for novel therapeutic strategies targeting biofilm eradication, and provide a predictive capability to accelerate the development of devices, water lines *etc.* that minimise microbial dispersal. Here our current understanding of biofilm mechanics is appraised from the perspective of biophysics, with an emphasis on constitutive modelling that has been highly successful in soft matter. Fitting rheometric data to viscoelastic models has quantified linear and non-linear stress relaxation mechanisms, how they vary between species and environments, and how candidate chemical treatments alter the mechanical response. The rich interplay between growth, mechanics and hydrodynamics is just becoming amenable to computational modelling and promises to provide unprecedented characterisation of infectious biofilms in their native state.

1 Introduction

The majority of chronic infections are due to sessile, surface-associated microbial communities known as biofilms [22, 40]. This protected mode of existence resists external challenges including many standard clinical treatments *via* a range of physiological and physical mechanisms, and this realisation is hastening the development of novel therapeutic strategies targeting biofilm-specific properties [7, 103]. Infectious biofilms may grow directly on tissue, but are also to be found attached to the surfaces of implanted devices where they are responsible for the majority of hospital-related infections [83]. Additionally, the transmission of pathogens

David Head
School of Computing, University of Leeds, UK. e-mail: d.head@leeds.ac.uk

between individuals is facilitated by transport through artificial water lines and airways where biofilms lay dormant, detaching cells under a combination of genetic control and flow-imposed mechanical stresses to colonise new biofilms downstream [16, 38]; see Fig. 1.

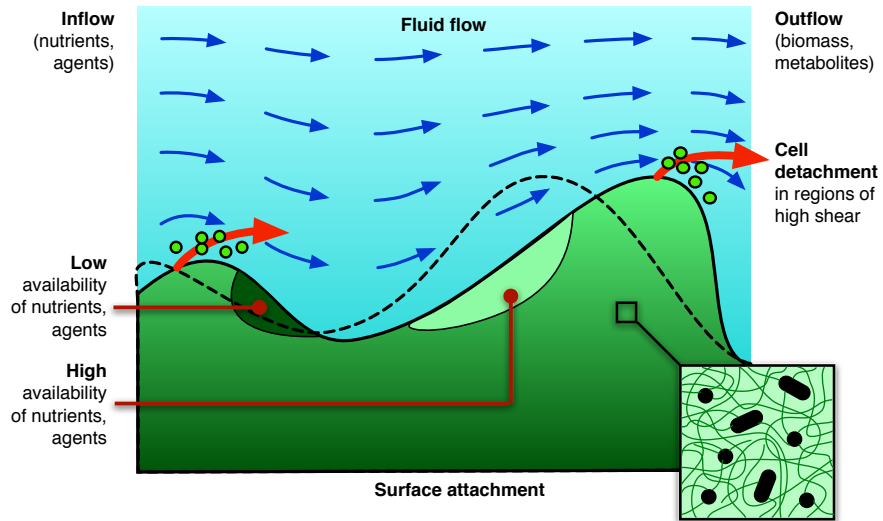


Fig. 1 Schematic representation of some issues relevant to biofilm mechanics. Fluid flow generates shear stresses that deforms the biofilm (solid) from its nominal unstressed profile (dashed line). Cellular detachment due to high shear stress is one mechanism for dispersal (large arrows). The direction of flow is modulated by the free surface, resulting in a non-uniform advection of dispersed phases such as nutrients, chemical agents, and metabolic products. Their availability therefore varies across the deformed biofilm profile. At a microscopic level, the mechanical properties ultimately derive from microbial cells and the polymeric matrix they produce (inset).

In many applications the expansion, detachment, and ultimately dispersal of potentially pathogenic microbes depends in part on the mechanical properties of their biofilm phenotype. This is perhaps most familiar in our daily attempts to reduce the bacterial load of the most accessible and well-studied biofilm of relevance to human health, dental plaque, by regular brushing [59, 97]. Other shear-based removal devices include microbubble jets for oral hygiene [46], and automated wipers [33] and wall-scraping ‘pigs’ [91] in industry. An integrated removal strategy first exposes biofilms to sublethal concentrations of antibiotics or other chemical agents, which can lead to reduced stiffness and enhanced removal, although crosslinkers and multivalent ions can increase stiffness [55, 106]. In addition, modifying the topographic, chemical or elastic properties of abiotic surfaces can reduce cell attachment or promote weak bonding that can be more easily removed [13, 24, 33, 35, 49].

Biofilm mechanics is not just important under physical brushing or scraping, however. Hydrodynamic flow is known to affect biofilm formation and propagation in dental unit water lines [100], catheters (both urinary tract and intravascu-

lar) and hemodialysis machines [36, 50, 83, 103], bile drains, stents, and voice prostheses [16]. In addition, the response to surface airflow and known airborne dispersal modes should be considered in the design of nosocomial ventilation systems [38, 83]. Flow is also a key consideration for industrial biofilms as overgrowth can cause clogging in biofilm reactors [52, 93], although here the goal is to maximise metabolic efficacy rather than microbial eradication.

The aim of this chapter is to summarise our current understanding of biofilm mechanics from the perspective of biophysics, in the hope of informing future investigations targeting the control or elimination of infectious biofilms under mechanical challenge. The primary distinction from a recent review [39] is the focus here on constitutive modelling following an approach common to soft matter systems, *i.e.* solutions of macromolecules such as colloids, flexible and semi-flexible polymers, which have been recognised as an abiotic counterpart of biofilms with regards mechanical response [102]. A pragmatic benefit of deriving and validating quantitative models is their predictive capability, which can be used to guide the design of novel technologies targeting reduced biofilm-related infections, for instance water lines that minimise microbial spread. However, the advantages of constitutive modelling go beyond characterisation. Identifying the relevant microscopic mechanisms responsible for observed bulk macroscopic behaviour generates fundamental insights with potentially far-reaching consequences, for instance in suggesting targets for novel therapeutics that would not otherwise have been considered, or allowing extrapolative predictions to situations not yet assayed experimentally. A wide range of theoretical and experimental methods have been developed over decades of soft matter physics research, and the potential benefits of porting these to the study of biofilms is substantial.

Biofilm mechanics is inherently a multi-disciplinary topic and as such there is a need to summarise a number of key concepts, some of which will undoubtedly already be known to readers. These are outlined in §2 with due apologies for any overfamiliarity of the material. It should be clearly stated from the outset what will *not* be considered here. The interactions between the microbes and the surface influence initial biofilm formation and generate adhesive complexes that need to be overcome or dismantled prior to large-scale motion or detachment [85, 96], but this important topic is simply too extensive to cover here. In addition, self-propelled bacterial swimmers are most commonly associated with the planktonic phenotype but are known to arise in some biofilms, both early stage and mature [45, 76], and could potentially be tractable to the analytical tools of active matter currently undergoing vigorous investigation [57], but since their relationship with biofilm mechanics has not been explored they will not be discussed further. The coupling between mechanics and community dynamics is likely to be of key importance in the future and is discussed in §4.

2 Background

In most situations biofilms are subjected to deformations or stresses that vary over length scales far exceeding that of the constituent molecules, making it impractical to characterise the mechanical response taking microscopic quantities as the degrees of freedom. It is often more expedient to adopt a coarse-grained continuum approximation defined by spatio-temporally averaged fields, much as the equations for hydrodynamics involve fluid velocity and density rather than the atomistic quantities from which they derive. In this section, some relevant aspects of continuum mechanics are briefly overviewed, followed by a survey of the primary experimental tools employed to quantify them *in vitro*. It is nonetheless important to remain mindful of the microscopic basis for these macroscopic quantities, and these will be discussed first.

2.1 Molecular origins of biofilm mechanics

From a physical perspective, biofilms can be crudely described as two-component systems comprising cells of various well-defined forms (spheres, rods *etc.*) embedded in a hydrated polymeric mesh [90]. If the volume fraction ϕ occupied by the cells is high, greater than roughly 0.2-0.5, the mechanical response will be dominated by steric hinderance acting between the stiff cell walls, and an analogy with colloidal systems is possible [102]. More commonly, however, $\phi \ll 1$ and the response is determined by the interdispersed matrix which reacts *via* purely physico-chemical mechanisms on times scales shorter than the cells' metabolic response. It is on these time scales that the analogy with abiotic systems is closest.

The multi-functional biofilm matrix consists of a variety of polysaccharides, extracellular DNA, proteins (including amyloid fibrils, *e.g.* curli), biosurfactants, and other macromolecules, with the composition depending on the cell strains and their environment [11, 34]. Its cohesive properties derive from chemical and strong physical intermolecular bonds (*e.g.* covalent, ionic) that are permanent on relevant time scales, and weak physical bonds (*e.g.* hydrogen bonds, van der Waals) with energies comparable to or less than the thermal scale $k_B T$ and are thus transient [78]. This description is strongly reminiscent of polymer solutions and gels, whose mechanical properties are well understood after decades of study in an industrial context [25, 78]. Following the established procedure outlined in Fig. 2, the bulk mechanical response can be theoretically derived by summing the force-extension curves for individual polymers over a hypothesised molecular composition. These force-extension relations derive from thermodynamic relations if thermal fluctuations are thought to dominate, or by treating polymers as slender elastic bodies if only enthalpic contributions (*e.g.* backbone stretching) are relevant.

Compared to flexible synthetic polymers, biopolymers can be thick, of the order of 1–10 nm or more [1], and this imbues them with a natural resistance to bending which significantly modifies their dynamics [65]. A highly successful force-

extension relation deriving from the wormlike chain (Kratky-Porod) model has been shown to describe well a range of biomolecules, including DNA [84], collagen [19], intermediate filaments [56] and actin [15, 73]. Incorporating increases in backbone length produces the extensible wormlike chain model applicable for large (*i.e.* non-linear) deformations [88]. Note that closed-form analytical expressions require multiple assumptions to be made, including the *affine* assumption that the local deformation field is a scaled-down version of the bulk strain [9, 15]. Spatially-extended models can relax such assumptions but typically require numerical solution.

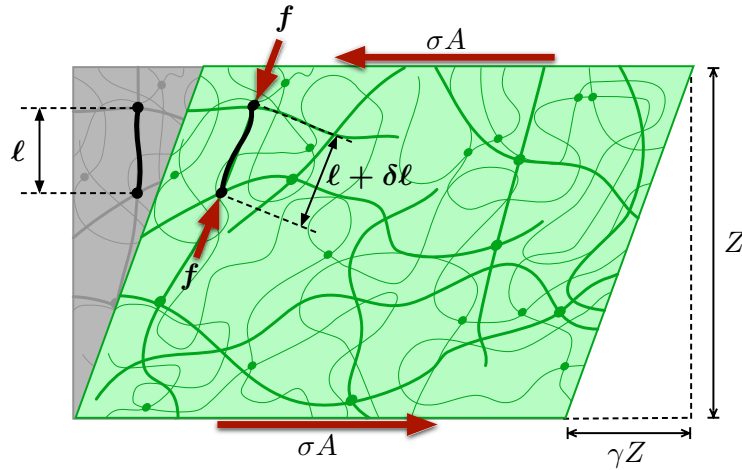


Fig. 2 A conceptual representation of a small volume of biofilm matrix under an imposed shear strain γ . The lines and nodes in the background (pre-strain) and foreground (post-strain) images correspond to polymers and inter-molecular interactions, respectively. The highlighted polymer segment extends from a length ℓ to $\ell + \delta\ell$ under the strain, resulting in equal-and-opposite tensile forces f acting on the nodes at each of its ends. Integrating over all such microscopic forces results in bulk forces σA acting across the body, with σ the shear stress and A the area of the opposing surfaces.

2.2 Continuum viscoelasticity

There are two central quantities in continuum mechanics; the stress, which is the force normalised to area and has units of pressure, and the strain or relative deformation which is dimensionless [8]. Both are properly rank-2 tensors [53], but for clarity only a scalar treatment in terms of the shear stress σ and shear strain γ will be discussed here (shear is usually chosen for soft matter systems as it is a volume-preserving mode that does not invoke solvent incompressibility). For a Hookean elastic body, $\sigma = G_0\gamma$ with G_0 the shear modulus, whereas a Newtonian fluid obeys $\sigma = \eta\dot{\gamma}$ with η the (shear) viscosity and $\dot{\gamma} \equiv d\gamma/dt$ the flow rate. Biofilms and soft

matter systems exhibit both behaviours simultaneously and are thus *viscoelastic*. Quantitative relationships between stresses and deformation variables are known as *constitutive equations*, of which $\sigma = G_0\gamma$ and $\sigma = \eta\dot{\gamma}$ are two examples, and deriving these relationships is the goal of the analytical coarse-graining procedure discussed in §2.1. Thus fitting validated constitutive equations to experimental rheometry data generates estimates of microscopic parameters in what can be thought of as a ‘rheological microscope’.

A key issue to identify early on is whether or not the material response is linear, *i.e.* if all stresses, strains and their time derivatives obey proportionality relations [8]. If linearity holds, the stress at time t can be written as the superposition of stresses due to infinitesimal strain increments $d\gamma = \dot{\gamma}(t) dt$ at all previous times,

$$\sigma(t) = \int_{-\infty}^t G(t-s)\dot{\gamma}(s) ds, \quad (1)$$

where $G(t)$ is the linear step-strain response [32, 78]. Alternatively, the strain at time t can be written as an integral over previous stress increments in terms of the compliance $J(t)$, where $J(t)$ gives the strain due to a step shear stress at $t = 0$ as measured in creep compliance tests [8]. As long as linearity holds, these two representations are equivalent [78]. Note that (1) assumes time translational invariance which would not hold if the material properties varied over the measurement time, when at least one additional time variable would be required [32].

To quantify the linear response at a particular frequency, it is common to apply an oscillatory shear $\gamma(t) = \gamma_0 \cos(\omega t)$ and measure components of the stress response that are in phase ($\propto \cos \omega t$) or out of phase ($\propto \sin \omega t$) with this driving. As shown in Fig. 3, this produces two moduli, the in-phase storage modulus $G'(\omega)$ and the out-of-phase loss modulus $G''(\omega)$. To avoid a proliferation of trigonometric functions it is expedient to adopt the complex representation $\gamma(t) = \text{Re}\{\gamma_0 e^{i\omega t}\}$, where ‘Re’ takes the real part. Inserting this into (1) gives

$$\sigma(t) = \text{Re}\{\gamma_0 G^*(\omega) e^{i\omega t}\}, \quad G^*(\omega) = i\omega \int_0^{\infty} e^{-i\omega t} G(t) dt, \quad (2)$$

where $G^*(\omega) = G'(\omega) + iG''(\omega)$. The entirety of a material’s linear response (for scalar shear) is contained in the two viscoelastic spectra $G'(\omega)$ and $G''(\omega)$. Examples are given in Fig. 3(b), including an elastic solid with $G'(\omega) = G_0$ and $G''(\omega) = 0$, and a viscous fluid obeying $G'(\omega) = 0$ and $G''(\omega) = \eta\omega$ (alternatively, $G^*(\omega) = G_0$ and $G^*(\omega) = i\eta\omega$ respectively). Just as the Hookean solid and Newtonian fluid represent idealised elastic and viscous bodies, schematic models have been devised for idealised viscoelastic materials, including the Maxwell model which relaxes to a viscous liquid over a single relaxation time, and the Kelvin-Voigt model which relaxes to an elastic solid [8]. Such schematic models are known as spring-dashpot models as they can be represented as combinations of (elastic) springs and (viscous) dashpots in serial, parallel, or both.

When linearity does not hold, superposition (1) is not valid, the various definitions of stress and strain tensors start to deviate [67], and both quantifying and mod-

elling the material response becomes more challenging. It is common to consider continuous shear $\gamma(t) = \dot{\gamma}t$ when investigating the non-linear response, although small-amplitude oscillatory shear about a fixed prestrain has also been employed for viscoelastic solids [88]. The non-linear regime is of most practical interest as stress-based detachment and failure are both non-linear phenomena, and for this reason the majority of biofilm rheology studies have focussed on this regime (see §3 below). Without supporting modelling, however, it is difficult to gauge the generality of reported findings with regards varying strains or environmental conditions. Successful predictive modelling for strongly deformed polymeric systems typically follows validation of linear models for the same material [25, 88], suggesting that pursuing a similar progression for biofilms would lead to representative constitutive equations for both the linear and non-linear response.

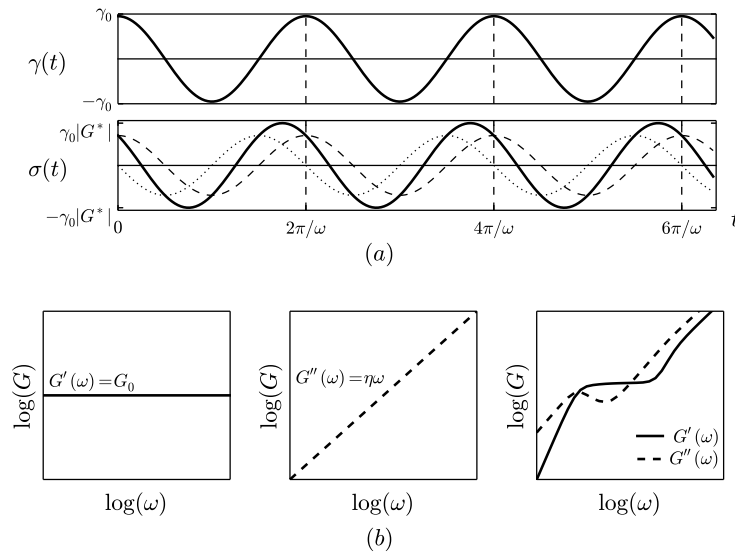


Fig. 3 (a) Example of an applied oscillatory shear strain $\gamma(t) = \gamma_0 \cos \omega t$ and the induced shear stress $\sigma(t)$, which can be decomposed into the in-phase contribution $\gamma_0 G'(\omega) \cos \omega t$ (dashed line) and the out-of-phase contribution $-\gamma_0 G''(\omega) \sin \omega t$ (dotted line). (b) Examples of viscoelastic spectra for a Hookean solid (left), a Newtonian fluid (middle), and an entangled solution of semi-flexible polymers [65] (right). Solid lines are $G'(\omega)$ and dashed lines are $G''(\omega)$.

2.3 Experimental biofilm rheology

The nature of biofilms renders the application of standard rheology measurement protocols problematic. Biofilms are thin, surface-associated, living colonies that

cannot be removed from their native environment without risk of altering their properties. They are also strongly heterogeneous, typically exhibiting a complex three-dimensional morphology with structured cell-rich and cell-deficient domains, the latter permitting flow [87, 99]. Measuring their mechanical properties has required modification of existing methods, or the development of novel biofilm-specific ones. Some commonly used methods are summarised below; for a more extensive discussion see [39].

Macrorheometry: Standard rheometers constrain the sample between two surfaces of various geometries (parallel plate, cone and plate, Taylor-Couette cell *etc.*), with the motion of one controlled to impose a predefined strain or stress schedule. Biofilms can be grown *ex situ* and transplanted to the rheometer, either intact on plates [41, 66] or by a destructive process [55, 104], or the rheometer modified to permit growth *in situ* [69, 70]. Macrorheometry can extract bulk properties [68, 82] but is not well suited to studying heterogeneities.

Macro and micro-indentation: The free surfaces of biofilms in their native state can be compressed globally [41, 71], or locally such as performed by atomic force microscopy [14, 54], and force-displacement relations and relaxation curves measured. Heterogeneity can be probed by multi-site sampling [48].

Microrheology: This methodology can be active or passive, and one or two particle [64]. For one particle, the motions of micron-scale particles undergoing passive Brownian motion are converted to $G^*(\omega)$ or $J^*(\omega)$ using thermodynamic relations [31, 61, 62], or they are actively driven *via* external forces and the moduli extracted directly [37, 106]. These particles are either added, or are endogenous such as the cells themselves [76]. Two-particle microrheology tracks correlated motion to reduce artefacts at the particle surfaces. Microrheology is well suited to studying heterogeneities and has been widely used in soft matter.

Flow cells: Imaging biofilms grown *in situ* in continuous flow cells is of direct relevance to many applications [16]. Non-linear streamers often form in rapid flow [89], whose visually-determined deformation fields can be fitted to those of simple elastic bodies to estimate static moduli [6, 90]. More recently, microfluidic devices have been employed to provide better environmental control and ensure laminar flow [52, 80, 86, 101], and fitting of visually-identified streamers [50] or partitioning walls [43] permits parameter estimation.

Biofilm reactors: Although industrially motivated, laboratory-scale attached growth reactors can be used to quantify the relationship between detachment and flow for generic biofilms, generating basic insight that may also apply to clinical situations. Reactor geometries are designed to expose high surface areas of the biofilm to flow, such as porous media [18, 99] or fibres [47, 94], and biomass effluent and other quantities measured.

3 Biofilm mechanics

The complex physical chemistry of biofilms, and in particular the multi-component biofilm matrix, makes it difficult to interpret rheology data in terms of identifiable microscopic processes. Even restricting attention to just the linear response regime still leaves a range of inter-molecular bonds or junctions that need to be considered to reproduce the full viscoelastic spectra $G'(\omega)$ and $G''(\omega)$. A common approach has been to fit rheometric data to a small number of viscoelastic constitutive equations, tracking parameter changes as microbial species, environmental conditions *etc.* are varied, but the proposed mechanisms underlying each fit remain unproven without independent measurements to confirm model validity. These problems are exacerbated in the non-linear regime, where additional processes such as cellular rearrangement must also be considered. A summary of our current understanding of biofilm rheology is presented here, starting with the bulk response before turning to consider more applied protocols.

3.1 Bulk rheology

$G'(\omega)$ and $G''(\omega)$ have been measured for biofilms of the well-characterised bacterium *P. aeruginosa* [29, 55] with similar results emerging from both studies, *i.e.* a weak frequency dependence over the range 10^{-3} Hz to 10 Hz, with a slight decay at low frequencies. Although $G'(\omega)$ was roughly an order of magnitude larger than $G''(\omega)$, indicating elastic-dominated behaviour, the two spectra became comparable on lowering the concentration of Ca^{2+} , suggesting a reduction in strong ionic matrix bonds and increased fluidity, consistent with fits to a superposition of wormlike chains [29]. Broadly similar spectra have been observed in a range of polymeric gels, including peptide fibrils [74], block copolymers [77] and intermediate filaments [56]. F pilus producing *E. coli* biofilms, but not curli producing ones, have also been compared to actin protein gels based on active microrheology experiments [37]. *P. aeruginosa* biofilms rapidly stiffen for frequencies exceeding 10 Hz [55], an effect not seen in the other systems mentioned.

Fitting stress relaxation in compressed biofilms to a generalised Maxwell model has been used to infer the relevance of extracellular DNA to the viscoelasticity of single species *S. mutans*, *P. aeruginosa*, *S. aureus* and *S. epidermidis* systems, where principal component analysis was employed to determine the number of modes [71]. Biomass rearrangement and flow modes were inferred from similar analysis of two oral species (*S. oralis* and *A. naeslundii*) and intact dental plaque [41]. Despite the intuitive appeal of these findings, it should be noted that spring-dashpot models are idealised and admit only a small number of relaxation times, in contrast to *P. aeruginosa* matrix extracts which have been shown to relax over a broad distribution of time scales [104]. Model-free data presentation in the form of $G'(\omega)$ and $G''(\omega)$ is preferable as it permits the development of theoretical tools subsequent to the

experimental study [29]. Spring-dashpot models are also linear, so their application to non-linear phenomena should only be attempted after careful consideration.

Quantifying changes in fit parameters as environmental factors are altered can identify controllable modifications leading to reduced stiffness and enhanced clearance. Parallel plate rheometry of *S. epidermidis* biofilms demonstrated a reduction in stiffness with increasing temperature, presumably by reducing the dissociation time for weak inter-molecular matrix bonds, with potential applications to medical devices [69]. Urea was found to weaken similar biofilms, possibly by interfering with hydrogen bonding [14]. Cellular growth under continuous flow resulted in stiffer biofilms for the same species, which may be a physiological response to sustained mechanical stress, although the failure strain did not significantly vary [4]. Antibiotics of sufficient concentration to destroy the majority of cells had no significant effect on the stiffness of the *E. coli* matrix, but it was drastically weakened by the protease trypsin, suggesting a dominant role for proteins in the matrix mechanics of this species [106]. By contrast, a broad range of chemical agents had no significant affect of the mechanics of *P. aeruginosa* biofilms, but could influence the rate of recovery from non-linear strains [55], possibly due to chemical modification of inter-molecular associations between matrix components.

These results highlight that different microbial species and strains produce different matrix polymers with broadly varying mechanical properties [5, 54], although commonality in the longest relaxation time has been claimed from linear creep fits in a parallel plate rheometer [82]. The non-linear response is also variable, with both shear thinning [55] and shear thickening [90] reported, although the empirical Cox-Merz rule relating linear oscillatory viscoelasticity to non-linear flow has been verified for *P. aeruginosa* matrix extracts [104] which, if found to be generally true, would aid the characterisation of biofilms in flow. An additional problem is the significant run-to-run variation, consistent with a broad, log-normal distribution [4], and the variation in stiffness, decreasing near the surface and increasing with age [37, 54, 76]. Such spatio-temporal variation can in principle be incorporated into suitably parameterised constitutive models, at the expense of an increased number of fit parameters and greater validation challenge.

3.2 *Fluid-structure coupling*

As shown in Fig. 1, the relationship between the deformation and growth of immersed biofilms and the shear stresses generated by the surrounding fluid flow is complex and bidirectional. Biofilm morphology influences local flow patterns and hence the fluxes of dispersed phases such as nutrients, metabolites, and quorum sensing molecules [86, 87, 101], and flow can drive biofilm morphogenesis to rippled beds [42, 89], streamers [80, 89, 90, 101], and rolling clusters [79]. The relevance of such process to the formation, growth, and dispersal of both infectious and non-infectious biofilms demands quantitative modelling with a predictive capability, but this situation is far from being realised. Even if a validated constitutive

model for the biofilm were available, its integration into these complex, dynamic geometries is challenging even with computational solution.

Partial insight can be attained by considering limited scenarios before tackling the full complexity. Streamers are elongated oscillating structures aligned with the flow direction that can form in turbulent conditions [89, 90] or in rapid laminar flow in microfluidic devices [80, 101], and can be visualised with optical or confocal microscopy and the profiles fitted to predictions for slender elastic filaments [6]. Note that fitting to elastic bodies only allows static quantities to be extracted, *i.e.* $G'(0) \equiv G_0$ and non-shear quantities such as the Poisson ratio [53] ($G''(0) \equiv 0$ by symmetry [8]). Modelling the two-way coupling between streamer elasticity and fluid flow presents numerical difficulties, but qualitative agreement has been reached in 2D, identifying vortices as the source of the oscillations [92]. An alternative reduced geometry is the lateral expansion of circular biofilms by osmosis (*i.e.* uptake of fluid into the matrix), for which good quantitative agreement between experiments and continuum modelling is possible [81]. Enhanced models have demonstrated that elastic instabilities can generate wrinkles, even without confinement [10, 30].

A complete description of a growing 3D biofilm in flow is only now becoming possible, but some modelling insight has already been achieved. Lattice models with cellular automata-like rules for biofilm growth have predicted a wide range of biofilm morphologies [75], and also graphically demonstrated the advection of substrates around the fluid-biofilm interface [72]. Continuum representations of the biofilm as constitutively linear elastic [21, 26, 28, 92], non-linear elastic [12, 27], viscous [20], or viscoelastic [95] bodies is challenging as the interface must be tracked using stress and displacement matching; simplifications such as a one-way coupling or reduced dimensionality are sometimes employed. Interface tracking is not required for phase field models, which have been employed to argue that low matrix elasticity is required for streamers to form [94] and to investigate the role of cohesion on interface stabilisation [51]. The non-overlapping range of feature sets and problems considered makes it difficult to discern a coherent picture from these modelling studies, but it is hoped that the advent of full-featured simulations (*e.g.* [21]) will herald reproducible investigations of an incrementally expanded parameter space generating consistent predictions for experiments.

3.3 Mechanically-induced detachment

Dispersal is part of the biofilm life cycle and as such under a degree of genetic control [63], but mechanics also plays a role. The inter-polymeric bonds that provide the matrix with its mechanical resilience and structural integrity must either be separated from cell surface proteins, enzymatically lysed, or overcome by tensile forces deriving from the external fluid shear [40], before cells can escape the biofilm envelope. Erosion of single cells, multi-cellular clusters (which maintain their resistance

to antibiotics [36]) and sudden large-scale sloughing events also result from fluid shear [23], limiting biofilm thickness [18].

Detachment is a key issue for industrial biofilm reactors and has been widely studied in this context. Reactors maximise the area of contact between microbes and fluid by growing the biofilms on highly porous supports, but this entails the risk of overgrowth leading to reduced flow rates and eventual blockage. Quantifying biomass effluent from complex biofilms grown in a glass-bead reactor in terms of a spatially-averaged model has revealed design principles that could be exploited to control growth and detachment [18]. Spatially-extended models reveal a complex biomass distribution on the scale of reactor pores, with reduced nutrient availability and biofilm growth downstream from clogged pores [52, 93]. A suite of techniques has been employed to measure velocity profiles and metabolic fluxes in terms of biofilm age and microbial composition [47], generating a range of data that could be used to validate highly sophisticated and predictive models.

Early models for shear-based detachment imposed height-dependent rates rather than solve for the explicit hydrodynamic flow field [2], but still demonstrated that combining multiple detachment mechanisms can generate a variety of morphologies [17]. To consider the effects of flow, some continuum fluid-structure coupling models have been extended to include detachment as reduced interfacial growth [21, 26] or a critical stress threshold [12, 72], and suggest erosion smoothens while sloughing roughens the biofilm surface. Note that not all of these include a two-way coupling between biofilm mechanics and fluid shear stress. Single-cell detachment events are best modelled using particle-based methods, but these do not typically include elasticity. One that does is the immersed boundary method in which the biofilm is represented as a spring-node assembly [3, 98], but this requires extension to include growth and dispersed-phase advection. Another is an off-lattice method from soft matter physics known as dissipative particle dynamics that has been applied to 2D biofilms [105], and includes thermal fluctuations of cells within the matrix which has been experimentally measured [76] but is often neglected in cell-scale models.

4 Outlook

Constitutive modelling of biofilm viscoelasticity, and in particular that of the biofilm matrix, provides quantitative insight into the mechanisms by which microscopic modifications cascade up through the length scales to influence the bulk properties relevant to the dispersal and removal of infectious colonies. Linear analysis is the most amenable to mathematical modelling and has already been employed as a tool to extract the importance of different inter-molecular interactions, as well as representing a first step towards fully non-linear models relevant to dispersal. Validated models can be employed to accelerate the design of treatments that beneficially modulate biofilm mechanics, and optimise the geometries of fluid transport systems to minimise microbial spread, to give just two examples. While it is clear that the

multi-component matrix represents a greater analytical challenge than classical soft matter systems, the difference is one of quantity rather than quality: Each intermolecular interaction can be modelled in isolation, the goal is to combine them into a comprehensive picture. This is most immediately possible in the linear regime where superposition applies.

While there has already been an array of investigations into specific pathogens, geometries and applications, progress towards a synthesis embracing biofilm mechanics and environmental conditions in general has been comparatively subdued. Whereas this may reflect the scope and complexity of the problem, the significant benefits of uncovering commonalities, such as the transferal of insight and analytical tools between problems, suggests such higher-level investigations deserve more attention. Overlapping studies would increase the chances of discovering such commonalities while helping to identify hidden relevant parameters that need to be controlled for reproducibility and hence predictability. This emphasis on universal properties is perhaps indicative of a physics viewpoint and will therefore only provide partial insight into biological problems, but as part of an integrated biophysical approach promises to reveal fundamental, general principles that will both elucidate biofilm mechanics and guide the development of future, robust treatments.

One aspect of natural biofilms not addressed here is that they are properly regarded as ecosystems, *i.e.* communities of different species and strains interacting with each other and their environment, including the host [22]. This is established for oral biofilms, where the ecological plaque hypothesis asserts that dental caries (tooth decay) results from excessive dietary carbohydrates promoting the overgrowth of acid-producing bacteria, and the resulting drop in pH promotes enamel demineralisation [58]. A similar picture has been argued for periodontal (gum) disease [60] (note that, according to Koch's postulates [44], these are *not* infections as the causative agents are present in healthy plaque, albeit in small numbers). Multi-species biofilms present different mechanical properties than their single-species counterparts [48], and therapies targeting mixed biofilms must ensure they do not preferentially remove commensal species, as this could conceivably lead to regrowth with an increased pathogenic fraction. Given the potential for mechanically altering the composition of infectious biofilms to reduce the numbers of pathogenic microbes, this fascinating and potentially rich coupling surely deserves greater attention.

Acknowledgement: DAH is funded by the Biomedical Health Research Centre, University of Leeds, UK.

References

1. *Molecular Biology of the Cell*, 5th ed., B. Alberts, A. Johnson, J. Lewis, M. Raff, K. Roberts, P. Walter (Garland, 2008).
2. E. Alpkvist, C. Picioreanu, M.C.M. van Loosdrecht, A. Heyden, *Biotech. Bioeng.* **94**, 961 (2006).

3. E. Alpkvist, I. Klapper, *Water Sci. Tech.* **55**, 265 (2007).
4. S. Aggarwal, R.M. Hozalski, *Langmuir* **28**, 2812 (2012).
5. S. Aggarwal, E.H. Poppele, R.M. Hozalski, *Biotech. Bioeng.* **105**, 924 (2010).
6. N. Aravas, C.S. Laspidou, *Biotech. Bioeng.* **101**, 196 (2008).
7. *Control of Biofilm Infections by Signal Manipulation*, ed. by N. Balaban (Springer, Berlin, 2008).
8. *An Introduction to Rheology*, H.A. Barnes, J.F. Hutton, K. Walters (Elsevier, 1989).
9. A. Basu, Q. Wen, X. Mao, T.C. Lubensky, P.A. Janmey, A.G. Yodh, *Macromolecules* **44**, 1671 (2011).
10. M. Ben Amar, M. Wu, *Europhys. Lett.* **108**, 38003 (2014).
11. L.P. Blanco, M.L. Evans, D.R. Smith, M.P. Badtke, M.R. Chapman, *Trends Microbiol.* **20**, 66 (2012).
12. M. Böl, R.B. Möhle, M. Heasner, T.R. Neu, H. Horn, R. Krull, *Biotech. Bioeng.* **103**, 177 (2009).
13. R.F. Brady, I.L. Singer, *Biofouling* **15**, 73-81 (2000).
14. E.R. Brindle, D.A. Miller, P.S. Stewart, *Biotech. Bioeng.* **108**, 2968 (2011).
15. C.P. Broedersz, F.C. MacKintosh, *Rev. Mod. Phys.* **86**, 995 (2014).
16. H.J. Busscher, H.C. van der Mei, *Clin. Microbiol. Rev.* **19**, 127-141 (2006).
17. J.D. Chambless, P.S. Stewart, *Biotech. Bioeng.* **97**, 1573 (2007).
18. H.T. Chang, B.E. Rittmann, D. Amar, R. Heim, O. Ehlinger, Y. Lesty, *Biotech. Bioeng.* **38**, 499 (1991).
19. S.-W. Chang, M.J. Buehler, *Materials Today* **17**, 70 (2014).
20. N.G. Cogan, *Int. J. Numer. Meth. Biomed. Engng.* **27**, 1982 (2011).
21. M. Coroneo, L. Yoshihara, W.A. Wall, *Biotech. Bioeng.* **111**, 1385 (2014).
22. J. W. Costerton, *The Biofilm Primer* (Springer, Berlin, 2007).
23. D.G. Davies, in *Biofilm Highlights*, ed. by H.-C. Flemming, J. Wingender, U. Szewzyk (Springer, Berlin, 2011).
24. S.C. Dexter, *J. Coll. Int. Sci.* **70**, 346-353 (1979).
25. *The Theory of Polymer Dynamics*, M. Doi, S. Edwards (Oxford, 1986).
26. R. Duddu, D.L. Chopp, B. Moran, *Biotech. Bioeng.* **103**, 92 (2009).
27. H.J. Dupin, P.K. Kitanidis, P.L. McCarty, *Wat. Res. Research* **37**, 2965 (2001).
28. H.J. Eberl, R. Sudarsan, *J. Theor. Biol.* **253**, 788 (2008).
29. A.E. Ehret, M. Böl, J. Roy. Soc. Int. **10**, 20120676 (2012).
30. D.R. Espeso, A. Carpio, B. Einarsson, *Phys. Rev. E* **91**, 022710 (2015).
31. R.M.L. Evans, M. Tassieri, D. Auhl, T.A. Waigh, *Phys. Rev. E* **80**, 012501 (2009).
32. S.M. Fielding, P. Sollich and M.E. Cates, *J. Rheol.* **44**, 323 (2000).
33. *Marine and Industrial Biofouling*, ed. by H.-C. Flemming, P. Sriyutha Murthy, R. Venkatesan, K.E. Cooksey (Springer, Berlin, 2009).
34. H.-C. Flemming and J. Wingender, *Nat. Rev. Microbiol.* **8**, 623 (2010).
35. J. Fu, Y.-K. Wang, M.T. Yang, R.A. Desai, X. Yu, Z. Liu, C.C. Chen, *Nat. Meth.* **7**, 733-736 (2011).
36. C.A. Fux, S. Wilson, P. Stoodley, *J. Bacteriol.* **186**, 4486 (2004).
37. O. Galy, P. Latour-Lambert, K. Zrelli, J.-M. Ghigo, C. Beloin, N. Henry, *Biophys. J.* **103**, 1400 (2012).
38. C.A. Gilkeson, M.A. Camargo-Valero, L.E. Pickin, C.J. Noakes, *Build. Env.* **65**, 35-48 (2013).
39. T. Guélon, J.-D. Mathias, P. Stoodley, in *Biofilm Highlights*, ed. by H.-C. Flemming, J. Wingender, U. Szewzyk (Springer, Berlin, 2011).
40. L. Hall-Stoodley, J.W. Costerton, P. Stoodley, *Nat. Rev. Microbiol.* **2**, 95 (2004).
41. Y. He, B.W. Peterson, M.A. Jongasma, Y. Ren, P.K. Sharma, H.J. Busscher, H.C. van der Mei, *PLoS ONE* **8**, e63750 (2013).
42. I. Hödl, L. Mari, E. Bertuzzo, S. Suweis, K. Besemer, A. Rinaldo, T.J. Battin, *Env. Microbiol.* **16**, 802 (2014).
43. D.N. Hohné, J.G. Younger, M.J. Solomon, *Langmuir* **25**, 7743 (2009).
44. *Essential Microbiology*, S. Hogg (Wiley, Chichester, 2005).

45. A. Houry, M. Gohar, J. Deschamps, E. Tischenko, S. Aymerich, A. Gruss, R. Briandet, Proc. Nat. Acad. Sci. **109**, 13088 (2012).
46. R.P. Howlin, S. Fabbri, D.G. Offin, N. Symonds, K.S. Kiang, R.J. Knee, D.C. Yoganantham, J.S. Webb, P.R. Birkin, T.G. Leighton, P. Stoodley, J. Dent. Res. **94**, 1303 (2015).
47. Z. Huang, E.S. McLamore, H.S. Chuang, W. Zhang, S. Werely, J.L.C. Leon, M.K. Banks, Biotech. Bioeng. **110**, 525 (2013).
48. G. Hwang, G. Marsh, L. Gao, R. Waugh, H. Koo, J. Dent. Res. **94**, 1310 (2015).
49. M.G. Katsikogianni, Y.F. Missirlis, Acta Biomaterialia **6**, 1107-1118 (2010).
50. M.K. Kim, K. Drescher, O.S. Pak, B.L. Bassler, H.A. Stone, New J. Phys. **16**, 065024 (2014).
51. I. Klapper, J. Dockery, Phys. Rev. E **74**, 031902 (2006).
52. C.E. Knutson, C.J. Werth, A.J. Valocchi, Wat. Res. Research **41**, W07007 (2005).
53. *Theory of Elasticity*, 3rd ed., L.D. Landau, E.M. Lifshitz (Butterworth-Heinemann, 1986).
54. P.C.Y. Lau, J.R. Dutcher, T.J. Beveridge, J.S. Lam, Biophys. J. **96**, 2935 (2009).
55. O. Lieleg, M. Caldara, R. Baumgärtel, K. Ribbeck, Soft Matter **7**, 3307 (2011).
56. Y.-C. Lin, N.Y. Yao, C.P. Broedersz, H. Herrmann, F.C. MacKintosh, D.A. Weitz, Phys. Rev. Lett. **104**, 058101 (2010).
57. M.C. Marchetti, J.F. Joanny, S. Ramaswamy, T.B. Liverpool, J. Prost, M. Rao, R.A. Simha, Rev. Mod. Phys. **85**, 1143 (2013).
58. P.D. Marsh, Adv. Dent. Res. **8**, 263 (1994).
59. P.D. Marsh, M.V. Martin, *Oral Microbiology*, 5th edn, (Churchill-Livingstone, 2009).
60. P.D. Marsh, A. Moter, D. Devine, Perio. 2000 **55**, 16 (2011).
61. T.G. Mason, Rheol. Acta **39**, 371 (2000).
62. T.G. Mason, D.A. Weitz, Phys. Rev. Lett. **74**, 1250 (1995).
63. D. McDougald, S.A. Rice, N. Barraud, P.D. Steinberg, S. Kjelleberg, Nat. Rev. Microbiol. **10**, 39 (2012).
64. D. Mizuno, D.A. Head, F.C. MacKintosh, C.F. Schmidt, Macromolecules **41**, 7194 (2008).
65. D.C. Morse, Macromolecules **31**, 7044 (1998).
66. J.-O. Ochoa, C. Coufort, R. Escudé, A. Liné, E. Paul, Chem. Eng. Sci. **62**, 3672 (2007).
67. *Non-linear Elastic Deformations*, R.W. Ogden (Dover, New York, 1984).
68. E. Paramonova, E.D. de Jong, B.P. Krom, H.C. van der Mei, H.J. Busscher, P.K. Sharma, App. Env. Microbiol. **73**, 7023 (2007).
69. L. Pavlovsky, R.A. Sturtevant, J.G. Younger, M.J. Solomon, Langmuir **31**, 2036 (2015).
70. L. Pavlovsky, J.G. Younger, M.J. Solomon, Soft Matter **9**, 122 (2012).
71. B.W. Peterson, H.C. van der Mei, J. Sjollem, H.J. Busscher, P.K. Sharma, mBio **4**, e00497-13 (2013).
72. C. Picioreanu, M.C.M. van Loosdrecht, J.J. Heijnen, Biotech. Bioeng. **72**, 205 (2001).
73. R.H. Pritchard, Y.Y.S. Huang, E.M. Terentjev, Soft Matter **10**, 1864 (2014).
74. D. Roberts, C. Rochas, A. Saiani, A.F. Miller, Langmuir **28**, 16196 (2012).
75. D. Rodriguez, B. Einarsson, A. Carpio, Phys. Rev. E **86**, 061914 (2012).
76. S.S. Rogers, C. van der Walle, T.A. Waigh, Langmuir **24**, 13549 (2008).
77. W.H. Rombouts, M. Colomb-Delsuc, M.W.T. Werten, S. Otto, F.A. de Wolf, J. van der Gucht, Soft Matter **9**, 6936 (2013).
78. *Polymer Physics*, M. Rubinstein, R.H. Colby (Oxford, 2003).
79. C.J. Rupp, C.A. Fux, P. Stoodley, App. Env. Microbiol. **71**, 2175 (2005).
80. R. Rusconi, S. Lecuyer, N. Autrusson, L. Guglielmini, H.A. Stone, Biophys. J. **100**, 1392 (2011).
81. A. Seminara, T.E. Angelini, J.N. Wilking, H. Vlamikas, S. Ebrahim, R. Kolter, D.A. Weitz, M.P. Brenner, Proc. Nat. Acad. Sci. **109**, 1116 (2012).
82. T. Shaw, M. Winston, C.J. Rupp, I. Klapper, P. Stoodley, Phys. Rev. Lett. **93**, 098102 (2004).
83. *The Role of Biofilms in Device-Related Infections*, ed. by M. Shirtliff, J. Leid (Springer, Berlin, 2009).
84. S.B. Smith, Y. Cui, C. Bustamante, Science **271**, 795 (1996).
85. F. Song, H. Koo, D. Ren, J. Dent. Res. **94**, 1027 (2015).
86. J.L. Song, K.H. Au, K.T. Huynh, A.I. Packman, Biotech. Bioeng. **111**, 597 (2014).
87. P.S. Stewart, Biofouling **28**, 187 (2012).

88. C. Storm, J.L. Pastore, F.C. MacKintosh, T.C. Lubensky, P.A. Janmey, *Nature* **435**, 191 (2005).
89. P. Stoodley, Z. Lewandowski, J.D. Boyle, H.M. Lappin-Scott, *Env. Microbiol.* **1**, 447 (1999).
90. P. Stoodley, Z. Lewandowski, J.D. Boyle, H.M. Lappin-Scott, *Biotech. Bioeng.* **65**, 84 (1999).
91. B. Szomolay, N.G. Cogan, *Env. Microbiol.* **17**, 1870-1883 (2015).
92. D. Taherzadeh, C. Piciooreanu, H. Horn, *Biophys. J.* **102**, 1483 (2012).
93. M. Thullner, P. Baveye, *Biotech. Bioeng.* **99**, 1337-1351 (2008).
94. G. Tierra, J.P. Pavissich, R. Nerenberg, Z. Xu, M.S. Alber, *J. Roy. Soc. Interface* **12**, 20150045 (2015).
95. B.W. Towler, A. Cunningham, P. Stoodley, L. McKittrick, *Biotech. Bioeng.* **96**, 259 (2007).
96. H.H. Tuson and D.B. Weibel, *Soft Matter* **9**, 4368 (2013).
97. M.J. Verkaik, H.J. Busscher, M. Rustema-Abbing, A.M. Slomp, F. Abbas, H.C. van der Mei, *Clin. Oral. Invest.* **14**, 403-409 (2010).
98. G.D. Vo, J. Heys, *Biotech. Bioeng.* **108**, 1893 (2011).
99. S.J. Vogt, A.B. Sanderlin, J.D. Seymour, S.L. Codd, *Biotech. Bioeng.* **110**, 1366 (2013).
100. J.T. Walter *et al.*, *Eur. J. Oral Sci.* **112**, 412-418 (2004).
101. W.M. Weaver, V. Milisavljevic, J.F. Miller, D. Di Carlo, *App. Env. Microbiol.* **78**, 5890 (2012).
102. J.N. Wilking, T.E. Angelini, A. Seminara, M.P. Brenner, D.A. Weitz, *MRS Bull.* **36**, 385-391 (2011).
103. *Medical Implications of Biofilms*, ed. by M. Wilson, D. Devine (CUP, Cambridge, 2003).
104. M. Wloka, H. Rehage, H.-C. Flemming, J. Wingender, *Coll. Poly. Sci.* **282**, 1067 (2004).
105. Z. Xu, P. Meakin, A. Tartakovsky, T.D. Scheibe, *Phys. Rev. E* **83**, 066702 (2011).
106. K. Zrelli, O. Galy, P. Latour-Lambert, L. Kirwan, J.M. Ghigo, C. Beloin, N. Henry, *New J. Phys.* **15**, 125026 (2013).